Respiratory Research

RESEARCH Open Access

A novel dual fixation method for improving the reliable assessment of pulmonary vascular morphology in pulmonary hypertension rats

Yan Xu[1†], Pu Liao[2,3*†], Xinyu Song[4*], Wenchuan Guo[1,3,5], Bingxun Liu[1,3], Tong Ye[1,3], Ting Zhang[3,6], Rui Xiao[1,3,5], Liping Zhu[1,3,5], Yujun Shen[7], Yanjiang Xing[8], Jing Wang[8] and Qinghua Hu[1,3,5*]

Abstract

This study introduced a novel dual fixation method for the pulmonary vasculature and lung tissue in pulmonary hypertension (PH) rats, addressing the limitations of traditional fixation methods that failed to accurately preserve the in vivo status of pulmonary vascular morphology. The modified method involved a dual fixation process, combining individualized ventilation support and vascular perfusion to simulate the respiratory motion, pulmonary artery pressure and right ventricular output of the rat under in vivo conditions. Utilizing a monocrotaline-induced PH rat model, this study compared the dual fixation with the traditional immersion fixation, focusing on the quantitative assessment of alveolar expansion degree, capillary patency, endothelial cell quantity and wall thickness of pulmonary vein and artery. The results demonstrated that the dual fixation is superior in maintaining the authenticity and integrity of lung tissue and more sensitive in the evaluation of pulmonary artery hypertrophy, providing a more reliable representation of pulmonary vascular remodeling associated with PH.

Keywords Lung tissue fixation, Pulmonary hypertension, Pulmonary vascular morphology

†Yan Xu and Pu Liao contributed equally to this work.

*Correspondence:
Pu Liao
luoshen166@163.com
Xinyu Song
songxinyu@ctgu.edu.cn
Qinghua Hu
qinghuaa@mails.tjmu.edu.cn
[1]Department of Pathophysiology, School of Basic Medicine, Tongji Medical College, Huazhong University of Science and Technology (HUST), 13 Hangkong Road, Wuhan 430030, China
[2]Department of Pathology, Union Hospital, Tongji Medical College, HUST, Wuhan 430022, China
[3]Key Laboratory of Pulmonary Diseases of Ministry of Health, Tongji Medical College, HUST, 13 Hangkong Road, Wuhan 430030, China
[4]Department of Respiratory and Critical Care Medicine, Affiliated Yichang Central People's Hospital of China Three Gorges University, Yichang 443003, China
[5]State Key Laboratory for Diagnosis and Treatment of Severe Zoonotic Infectious Diseases, HUST, 13 Hangkong Road, Wuhan 430030, China
[6]Department of Pulmonary and Critical Care Medicine, The Sixth Hospital of Wuhan, Affiliated Hospital of Jianghan University, 168 Hongkong Road, Wuhan 430000, China
[7]Department of Pharmacology, Tianjing Key Laboratory of Inflammatory Biology, School of Basic Medical Sciences, Tianjing Medical University, 22 Qixiangtai Road, Heping District, Tianjing 300070, China
[8]State Key Laboratory of Respiratory Health and Multimorbidity, Institute of Basic Medical Sciences, School of Basic Medicine, Chinese Academy of Medical Sciences, Peking Union Medical College, Beijing 100005, China

Introduction

Pulmonary hypertension (PH), characterized by elevated pulmonary artery pressure and vascular resistance leading to right heart failure, represents a serious challenge in respiratory and cardiovascular research [1, 2]. Pulmonary vascular morphology is necessarily evaluated to directly and quantitatively reflect pulmonary vascular remodeling [3, 4]. Nevertheless, the authenticity of this evaluation significantly depends on the method used for lung tissue fixation [5, 6].

Currently, lung tissue fixation methods include immersion fixation, intratracheal perfusion fixation, tracheal ligation fixation, vascular perfusion, in situ fixation, fixed volume fixation and vacuum inflation [5–12]. Immersion fixation involves completely submerging the lung tissue in a fixative to preserve the integrity of cells and the extracellular matrix [7]. Intratracheal perfusion fixation fixes lung tissue by directly injecting the fixative into the trachea, allowing the fixative to uniformly distribute throughout the alveoli and lung tissue, effectively maintaining the lung's structure and morphology [6, 8]. Tracheal ligation fixation involves tying off the trachea and directly introducing the fixative into the lungs through the trachea, which is especially effective in maintaining the lungs' natural expansion state and microscopic structure compared to intratracheal perfusion fixation [6]. Vascular perfusion introduces the fixative through the animal's vascular system to achieve rapid and uniform tissue fixation but is less conducive to preserving the structural integrity and morphological characteristics of the airways and alveoli [5, 6]. In situ fixation refers to fixing the tissue in its original position, with the fixative delivered directly to the lungs through the trachea to better preserve the lung tissue's natural state and microscopic structure [5, 9, 11]. In the fixed volume fixation method, lung tissue is fixed within a pre-set volume to help maintain the tissue's original shape and size [5, 10]. Vacuum inflation places lung tissue in a vacuum environment and then slowly introduces fixative or air into the lungs to simulate the natural expansion state of the lungs, maintaining the structure of alveoli and bronchioles [5, 12]. However, up until now, there is no fixation method specifically designed to preserve the morphology of both pulmonary vasculature and surrounding tissue including airways and alveoli, providing a more precise and realistic visualization and assessment of the alterations of pulmonary vascular morphology or remodeling associated with PH.

In this study, we explored a modified method involving a dual fixation process for the pulmonary vasculature and airways. We utilized monocrotaline (MCT) to induce PH in Sprague-Dawley (SD) rats [13], and compared the dual fixation with the traditional or simple immersion fixation on the integrity of lung tissue and pulmonary vasculature structure. The results indicated that the dual fixation method more effectively preserves the in vivo structure of lung tissue, particularly the authenticity and integrity of pulmonary vascular morphology, enabling detailed morphological analysis and more reliable description of PH pathological alterations.

Materials and methods

Ethics approval and animal housing

This study involved a total of 24 Sprague-Dawley rats, aged 7–8 weeks, with an equal distribution of males and females, each weighing approximately 200 g. These animals were approved for use by the Institutional Animal Care and Use Committee of Tongji Medical College, Huazhong University of Science and Technology. The rats were housed three per cage in a 0.3 m^3 enclosure and maintained under a 12-hour light/dark cycle with ad libitum access to standard laboratory chow and water. The bedding consisted of high-temperature autoclaved wood shavings, which were changed twice weekly. The source of rats was Hunan Slaque Jingda Laboratory Animal Co., LTD., SPF level. The rats were anesthetized via an intraperitoneal injection of 40 mg/kg sodium pentobarbital (1% solution).

Pulmonary hypertension model and hemodynamic measurements

The experimental animals were randomly divided into four groups, six animals per group, evenly split between males and females. Two groups received intraperitoneal injections of monocrotaline (MCT) at a dose of 60 mg/kg to establish the model group (MCT group) as described in previous studies [13, 14] including ours [14], while the other two groups were given intraperitoneal injections of saline to serve as the control group (control group). Twenty-one days later, the pulmonary hemodynamics including mean pulmonary arterial pressure (mPAP), cardiac output and systemic circulation pressure were measured using a PE-50 catheter and a thermosensitive probe for cardiac output, connected to a PowerLab signal acquisition system as fully reported in our previous studies [15–18].

Right ventricular hypertrophy measurements

The heart tissues were collected for trimming, the weight of the right ventricular wall (RV) and the left ventricular wall and septum (LV + S) were measured. Right ventricular hypertrophy was calculated as RV/(LV + S) [15–18].

Traditional lung tissue fixation-immersion fixation only

Following the pulmonary hemodynamic measurements, the rats were transferred to the operating table, where the chest cavity was fully exposed. An incision was made in the left atrium using ophthalmic scissors and both the

superior and inferior vena cava were clamped off. A 50 mL syringe with an infusion needle with a 0.6 mm diameter was inserted into the right ventricular wall towards the pulmonary artery, and saline was slowly infused until no blood flowed out from the left atrium. The left and right lungs were then removed, placed on filter paper to blot away excess fluid, and subsequently immersed in 4% paraformaldehyde for 24 h fixation before being embedded in paraffin [7].

Modified lung tissue fixation-dual fixation in ventilated and perfused lung

After completing the pulmonary hemodynamic measurements, the rat was moved to the operating table and the parameters of a ventilator (PhysioSuite, PS5677, Kent, USA) were pre-set according to rat weight. Additionally, a 500 mL saline solution was prepared in an infusion bottle with an infusion needle with a 0.6 mm diameter. The infusion bottle was set at the height of the liquid level in the infusion dripper as follows: the height (H) from the liquid level in the dripper to the rat heart (cmH_2O) = 1.36 × mPAP (mmHg) (Figure. S1). The vascular perfusion pressure was thus adjusted to the level equivalent to pulmonary artery pressure, the flow rate was adjusted to the level equivalent to the output. The purpose of the above adjustments was to simulate the pulmonary vascular perfusion status in intact rats for each. The trachea was isolated and a "V" shaped incision was made just below the laryngeal cartilage using ophthalmic scissors, followed by tracheal intubation and connection to the ventilator. When the respiratory rate matched the frequency of the ventilator's waveform settings, the thoracic cavity was exposed, and an incision was made at the left atrial appendage. The superior and inferior vena cava were clamped off, and an infusion needle was inserted into the right ventricular wall and placed in the pulmonary artery, a hemostat was then used to secure the needle in place. The vascular perfusion was conducted using the above settings until no blood flowed out of the left atrial incision. The infusion bottle was then replaced with another one containing 4% paraformaldehyde, maintaining the same height and perfusion rate for 2 min to fix the pulmonary vessels under the same conditions individually simulating pulmonary artery pressure and cardiac output in intact rats for each. The tracheal tube was removed, and 4% paraformaldehyde was slowly dropped into the trachea until it overflowed, the trachea and both pulmonary hilums were quickly ligated to prevent post-dissection airway collapse. The intact left and right lungs were then immersed in 4% paraformaldehyde for 24 h fixation before paraffin embedding and Hematoxylin and Eosin staining.

Alveolar mean linear intercept (Lm)

For each of the six animals in a group, one HE slide or section was prepared. From each slide, four 40× magnification fields (286 μm×158 μm for each) without large blood vessels and airways were chosen. Using Photoshop, a 65 grid of horizontal test lines (d) was overlaid. The left side served as the counting point, with the number of points at the left end of the alveolar cavity (p) and the number of intersections between the test lines and the alveolar septa (I) being counted. Lm was calculated using the formula Lm = 2 × [(d×p)/I] [19–22] (Figure. S2).

Pulmonary parenchymal volume density (Vv)

For each of the six animals in a group, one HE slide or section was selected. From each slide, four fields (286 μm×158 μm) at 40× magnification were chosen. Using Photoshop, a 5 × 8 grid of "cross" test lines was overlaid. Counting was based on the right upper quadrant, where intersections with the pulmonary parenchyma were counted. This process determined the total number of points falling on the pulmonary parenchyma (Pp) and the total number of test points within the field of view (PL). The volume density of the pulmonary parenchyma, Vv, was then calculated using the formula Vv = Pp/PL [19, 21, 23] (Figure. S3).

Alveolar septal thickness (T)

For each of the six animals in each group, one HE slide or section was selected. From each slide, four fields of view (286 μm×158 μm) at 40× magnification were chosen. Using Photoshop, five horizontal test lines were overlaid onto the image. The thickness of the pulmonary septa intersected by the test lines was measured, focusing specifically on those septa where the angle of intersection with the test line was greater than 60 degrees. This method ensures the measurement of septal thickness in a standardized manner, avoiding bias that might arise from measuring at shallow angles, which could artificially inflate thickness readings [19] (Figure. S4).

Alveolar diameter (R)

For each group consisting of six animals, one HE slide or section per animal was selected. Four fields of view from each slide and one alveolus from each field were randomly chosen for measurement of their diameters using Image Pro Plus software. This process ensures accurate measurement of the alveolar diameters by standardizing the procedure across all selected alveoli, facilitating the quantitative analysis of lung morphology.

Grouping of pulmonary vessels

For vessels with a diameter greater than 100 μm, the following features or criteria were used in this study to distinguish pulmonary arteries from veins: pulmonary

arteries exhibit smaller lumens, thicker and more uniform wall layers, and tend to have round or oval shapes. Conversely, pulmonary veins feature larger lumens, thinner wall layers, and more irregular shapes. For vessels with a diameter less than 100 μm, a series of features or criteria were used in this study to distinguish pulmonary arteries from veins as follows: (1) For vessels with a diameter less than 100 μm, the characteristics of parallel pulmonary arteries and veins are similar to those of vessels with a diameter greater than 100 μm. (2) Within the same tissue section, pulmonary arteries are stained slightly darker than pulmonary veins. (3) Pulmonary artery endothelial cells are denser and protrude into the lumen, compared to pulmonary veins. (4) Pulmonary vein endothelial cells are sparser and relatively flattened, bulging into the lumen. The scarcity of endothelial cells in lymphatic vessels and the presence of red blood cells within can exclude the possibility of lymphatic vessels. (5) The external membrane of pulmonary arteries is thicker than that of pulmonary veins and lymphatic vessels [24–27].

Intrapulmonary vascular wall thickness measurement and endothelial cell count

For each animal, one HE slide or section was selected, and the full image of the whole tissue was obtained by scanning the slide using (VS120, Olympus, Japan). The software Vista-scan was used to collect images of all vessels within the lung tissue. Subsequently, measurements of each vessel's inner and outer diameters were taken into Image Pro Plus software to calculate the thickness of the vascular wall by the formula: (outer diameter - inner diameter) ×100% / outer diameter [15–18]. Endothelial cell counting within pulmonary vessels was performed by calculating the endothelial cell nuclei lining the lumens of vessels with different diameters.

Cdh5 immunocytochemical staining and collapsed or opened capillaries

For the immunofluorescence staining, 5-μm-thick lung sections were incubated overnight at 4 °C with a mixture of Cdh5 antibody (1:300, Abbrab, Cat#ABF11356). After washing with PBS, the tissues were incubated with a fluorescent secondary antibody (1:300, Abcam, Cat#ab150113) at room temperature for 1 h. Fluorescence images were then acquired using a confocal laser microscope (Zeiss, LSM780, Oberkochen, Germany). The number of collapsed and open capillaries within a field (115 μm×95 μm) of total four fields for each slide was counted [28]. The ratios of opened and collapsed capillaries were calculated as follows: percentage of collapsed capillaries = (number of collapsed capillaries / total capillaries) × 100%, percentage of opened capillaries = (number of opened capillaries / total capillaries) × 100%.

Statistical analysis

Data was presented as Mean ± SEM. Normally distributed data was analyzed by Brown-Forsythe tests followed by ordinary One-ANOVA (equal variance test passed) or Welch ANOVA (equal variance test failed) post-hoc multiple groups comparisons. Non-normally distributed data was analyzed by Kruskal-Wallis tests followed by Dunn's multiple groups comparisons. The post hoc test of one-way ANOVA was divided into two cases, Fisher's LSD test was used when the variance was equal, and Dunnett's T3 ($n < 50$/group) or Games-Howell ($n > 50$/group) was used when the variance was not equal. GraphPad Prism (version 9.0) was employed for statistical analysis, considering P value<0.05 as statistically significant.

Results

Establishment of MCT-induced pulmonary hypertension model in rats

As compared to the control, MCT treatment induced significant increases in mPAP, PVR, and RV/(LV + S) ratio (Fig. 1A-C), indicating successful establishment of pulmonary hypertension in the rats. Furthermore, there were no statistically significant differences in the above parameters between the rats with lung tissue treated by immersion fixation or dual fixation (Fig. 1A-C), objectively enabling the subsequent comparison of the two fixation methods.

The better alveolar expansion in lung treated by dual fixation than immersion fixation

To reveal the impact of two fixation methods on the degree of alveolar dilation, we measured alveolar linear intercept, alveolar diameter, alveolar parenchymal volume density, and alveolar septal thickness. Alveolar linear intercept and alveolar diameter are used to evaluate the degree of emphysema, and as they are positively correlated with the degree of lung or alveolar expansion [19, 22]. The morphometric analysis showed significantly greater lung linear intercepts and alveolar diameter in lung treated by dual fixation than immersion fixation (Fig. 2B and C).

The lung parenchymal volume density (Vv) is the proportion of air-exchanging tissue per unit volume in the lung, used to evaluate the degree of lung consolidation [19, 21, 23]. The alveolar septum thickness can reflect the gas exchange capacity. Under physiological conditions, the thinner the lung diaphragm, the stronger the gas exchange capacity [19]. Therefore, the lung parenchyma volume density and the alveolar septum thickness indirectly indicate the degree of alveolar dilation [19, 21, 23]. The morphometric analysis identified significantly less Vv and alveolar septum thickness in lung treated by dual fixation than immersion fixation (Fig. 2D and E). As compared to control rats without MCT treatment, MCT

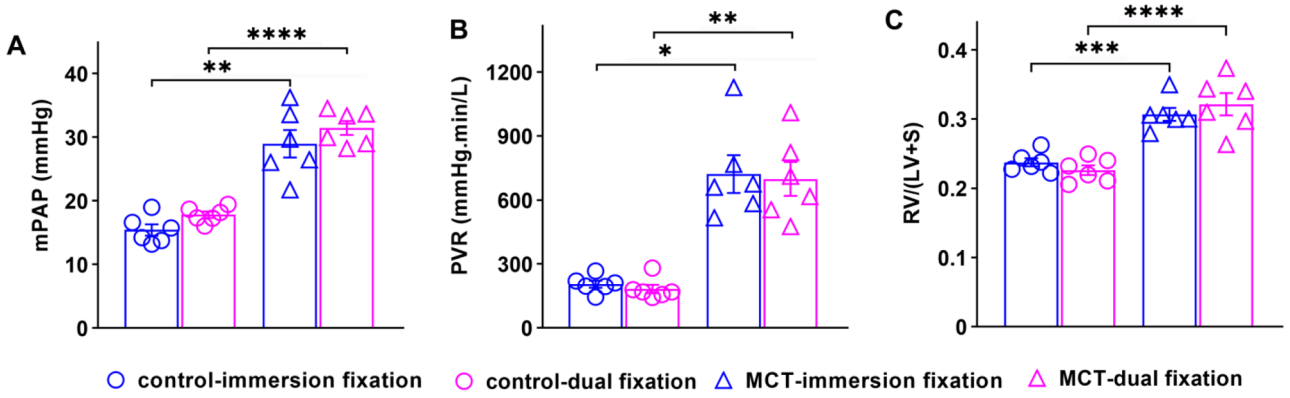

Fig. 1 The MCT-induced pulmonary hypertension and right ventricular hypertrophy in rats. The alterations of mean pulmonary artery pressure (mPAP, **A**), pulmonary vascular resistance (PVR, **B**), and right ventricular hypertrophy (RV/(LV + S), **C**), * $P < 0.05$, ** $P < 0.01$, *** $P < 0.001$, **** $P < 0.0001$, $n = 6$ for each group

treatment caused a significantly increase in alveolar septum thickness in rats with lungs treated either by dual fixation or by immersion fixation (Fig. 2E).

The above experimental results indicated that the dual fixation better preserves the structural integrity of the lung tissue in more close to its status in vivo.

The better capillary patency in lung treated by dual fixation than immersion fixation

To assess the effects of the fixation method on the patency of alveolar capillaries in rats, the classical endothelial marker, Cdh5 immunofluorescence staining was performed. As shown in Fig. 3A, representative images of lung sections visualized Cdh5-positive area without or with lumen as the collapsed and opened capillaries. Quantitative analysis revealed a significantly higher ratio of opened alveolar capillaries and lower ratio of alveolar collapsed capillaries in lung tissues treated by dual fixation as compared to immersion fixation (Fig. 3B-C). These results indicated that the dual fixation preserves capillary patency better than immersion fixation.

No difference in edothelial cell quantity in intrapulmonary vessels across varying diameters between dual fixation and immersion fixation

To evluate the effects of the fixation method on the integrity of endothelial cells in rat pulmonary vessels, we measured the endothelial cell counts in pulmonary vessels of different diameters across each group. There was no significant difference in the number of endothelial cells across different vascular diameters between dual fixation and immersion fixation in control rats without MCT treatment and in the rats with MCT treatment (Fig. 4A-C). As compared to the control rats without MCT treatment, significant reductions in endothelial cell counts were observed in MCT-treated rats either by dual fixation or immersion fixation (Fig. 4A-C). The results indicated that the fixation does not significantly impact the evaluation of integrity of pulmonary vascular endothelial cells in rats. However, the damage caused by MCT treatment was significant regardless of the dual or immersion fixation method used.

The lower wall thickness of intrapulmonary veins across varying diameters in dual fixation than immersion fixation

To compare the effects of fixation method on the wall thickness of intrapulmonary veins, we evaluated the wall thickness of intrapulmonary veins across three different diameters using both fixation methods. The intrapulmonary veins wall thickness in the dual fixation was substantially thinner as compared to the traditional immersion fixation in both control rats without MCT treatment and in the rats with MCT treatment (Fig. 5A-C). As compared to the control rats without MCT treatment, no significant alteration in intrapulmonary veins wall thickness was observed in MCT-treated rats either by dual fixation or immersion fixation (Fig. 5A-C).

The results suggested that the lung tissue fixation method has obvious impacts on the measurement of intrapulmonary vein wall thickness. The dual fixation demonstrated a notably lower wall thickness of intrapulmonary veins across various diameters as compared to the immersion fixation in both control and MCT-treated rats. Additionally, no change in intrapulmonary vein wall thickness was noted in the MCT-treated rats using either fixation method. Considering the overall better preservation of lung tissue by dual fixation, the wall thickness of intrapulmonary veins is over-estimated by immersion fixation across various diameters.

The lower wall thickness of the intrapulmonary arteries snug against trachea across varying diameters in dual fixation than immersion fixation

To examine the effect of fixation method on the thickness of intrapulmonary artery wall across different diameter, we measured the wall thickness of intrapulmonary

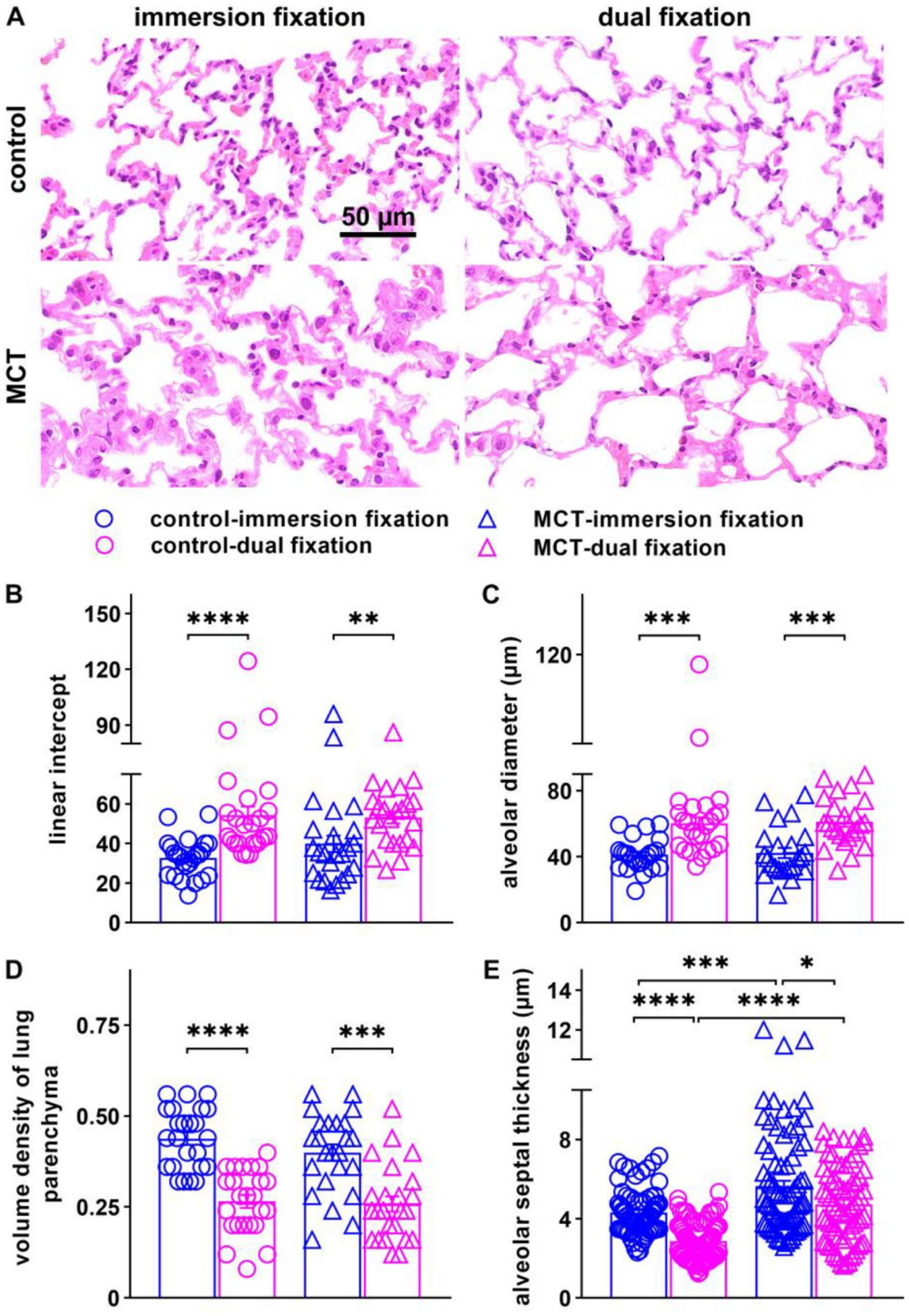

Fig. 2 The effects of fixation method on alveolar expansion. The representative imagings of HE-staining showing alveolar dilation in rats with lung tissue treated by immersion fixation or dual fixation with or without MCT treatment (**A**), and the statistical comparisons of alveolar linear intercept (**B**), alveolar diameter (**C**), lung parenchymal volume density (**D**) and alveolar septal thickness (**E**), * $P < 0.05$, ** $P < 0.01$, *** $P < 0.001$, **** $P < 0.0001$, $n = 6$ for each group

arteries snug against trachea. In this study, intrapulmonary arteries snug against trachea were defined as those where the vascular smooth muscle was in direct in contact with the tracheal smooth muscle, the intrapulmonary arteries classified histologically as bronchial arteries.

The intrapulmonary arteries snug against trachea (bronchial arteries) in the dual fixation was obviously thinner than immersion fixation in both control rats without MCT treatment and the rats with MCT treatment (Fig. 6A-B). As compared to the control rats

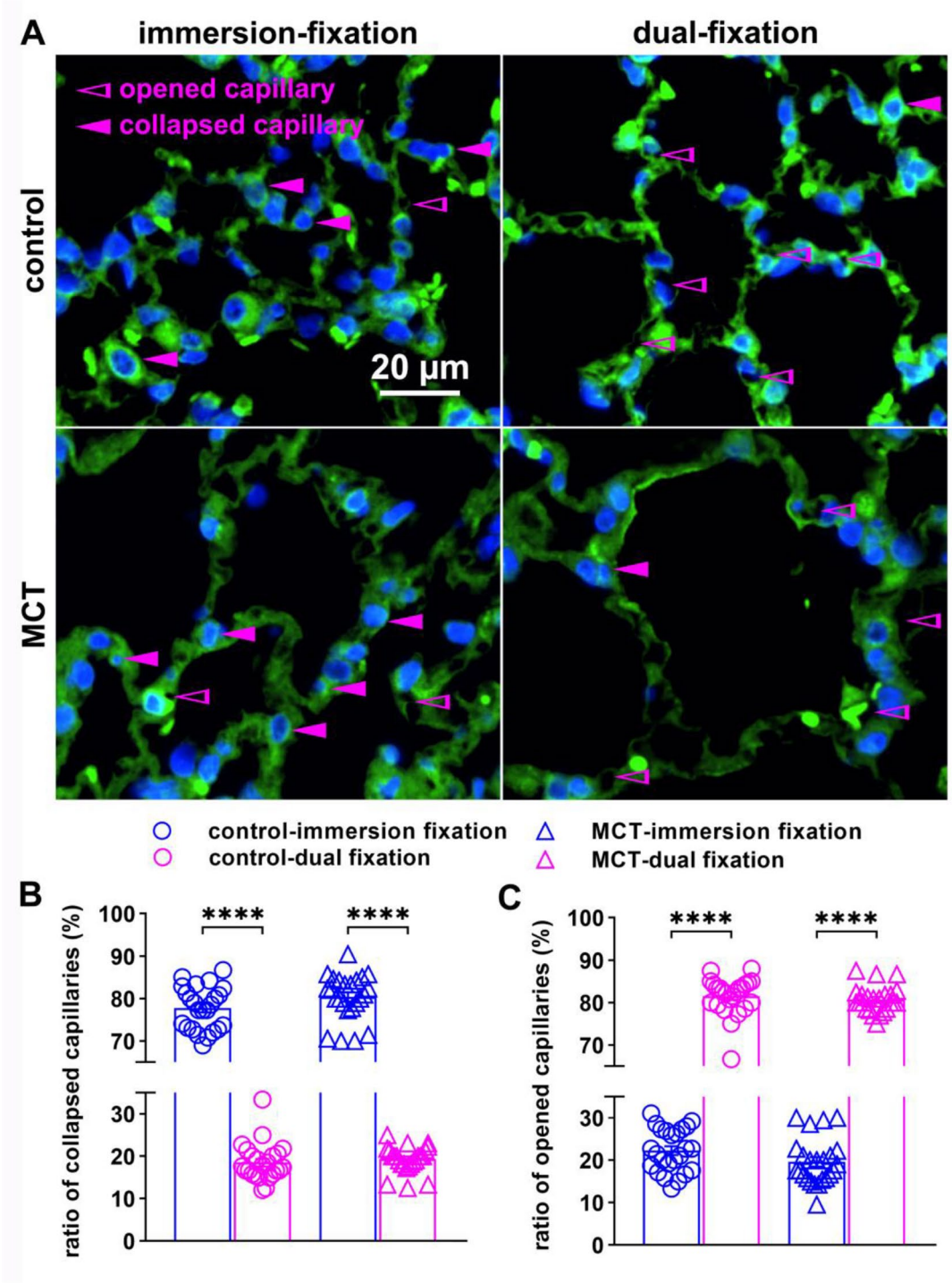

Fig. 3 The effect of fixation method on alveolar capillary patency. The representative images of Cdh5 immunofluorescence staining in lung tissue treated by immersion fixation or dual fixation (green for Cdh5 and blue for DAPI, **A**), and the statistical comparisons of the ratio of collapsed capillaries (**B**) and the ratio of opened capillaries (**C**). * $P < 0.05$, ** $P < 0.01$, *** $P < 0.001$, **** $P < 0.0001$, $n = 6$ for each group

without MCT treatment, no significant alteration in the wall thickness of intrapulmonary arteries snug against trachea was observed in MCT-treated rats either by immersion fixation or dual fixation (Fig. 6A-B).

The findings indicated that the choice of fixation method significantly influences the evaluation of wall thickness of intrapulmonary arteries snug against trachea (bronchial arteries) across varying diameters. Notably,

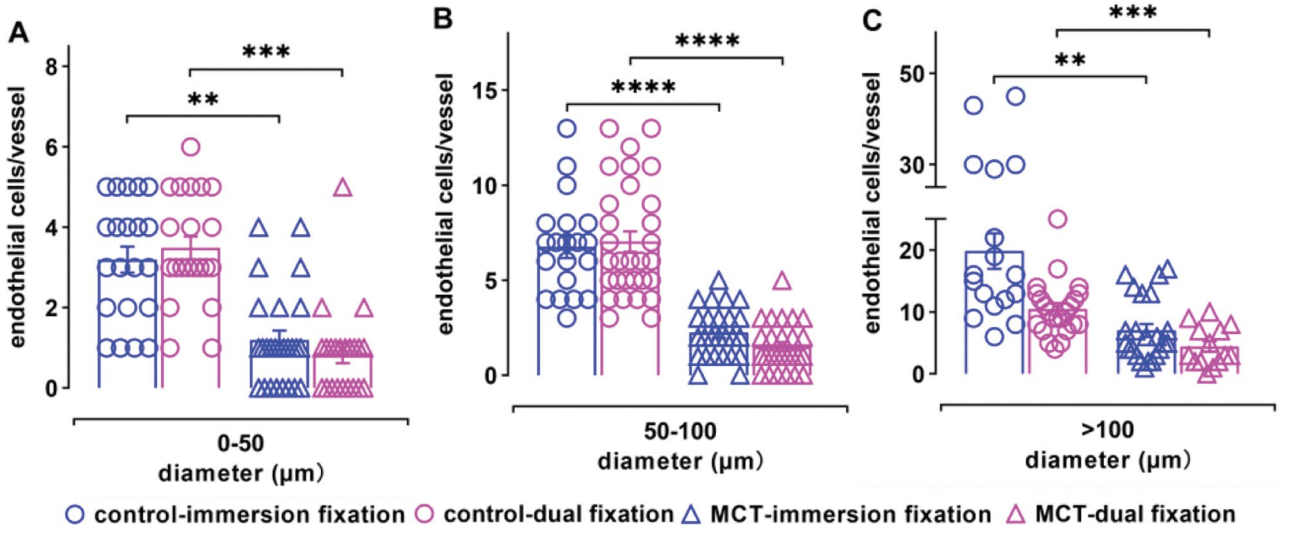

Fig. 4 The effect of fixation method on endothelial cell counts of intrapulmonary vessels across varying diameters. The statistical comparisons of endothelial cell counts in intrapulmonary vessels between immersion fixation and dual fixation in rats without or with MCT treatment (**A**-**C**), and between rats without or with MCT treatment by the same fixation method (**A**-**C**). * $P<0.05$, ** $P<0.01$, *** $P<0.001$, **** $P<0.0001$, $n=14$–30 pulmonary vessels from each of 6 rats for each group

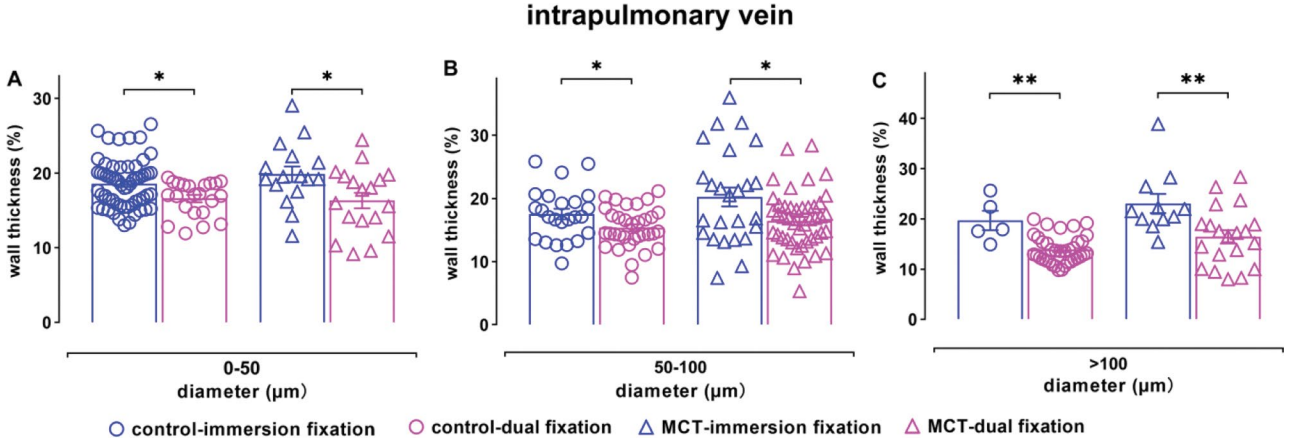

Fig. 5 The effect of fixation method on the evaluation of wall thickness of intrapulmonary veins across varying diameters. The statistical comparisons of wall thickness in intrapulmonary veins between immersion fixation and dual fixation in rats without or with MCT treatment (**A**-**C**), and between rats without or with MCT treatment by the same fixation method (**A**-**C**). * $P<0.05$, ** $P<0.01$, *** $P<0.001$, **** $P<0.0001$, $n=5$–59 pulmonary vessels from each of 6 rats for each group

the wall thickness in these arteries is over-estimated in immersion fixation as compared to dual fixation.

The more severe pulmonary artery hypertrophy revealed by dual fixation than immersion fixation

In this study, the intrapulmonary arteries away from the trachea mean the distance between intrapulmonary arteries and trachea was greater than 0 μm. The intrapulmonary arteries away from trachea by dual fixation were notably thinner than immersion fixation in both the control rats without MCT treatment and the rats with MCT treatment (Fig. 7A-C). As compared to the control rats without MCT treatment, a significant increase in the wall thickness of intrapulmonary arteries away from trachea, the pulmonary artery hypertrophy, was observed in MCT-treated rats either by dual fixation or immersion fixation (Fig. 7A-C). More importantly, the MCT-induced increase in the wall thickness of intrapulmonary arteries away from trachea, particularly those with diameter between 50 and -100 and > 100 μm, evaluated by dual fixation was more than immersion fixation (Fig. 7D). In other words, the dual fixation was more sensitive than immersion fixation in the estimation of pulmonary artery hypertrophy.

In summary, the fixation method affects the evaluation of wall thickness of intrapulmonary arteries away from the trachea across various diameters, with the lower wall thickness level and more severe hypertrophy induced by

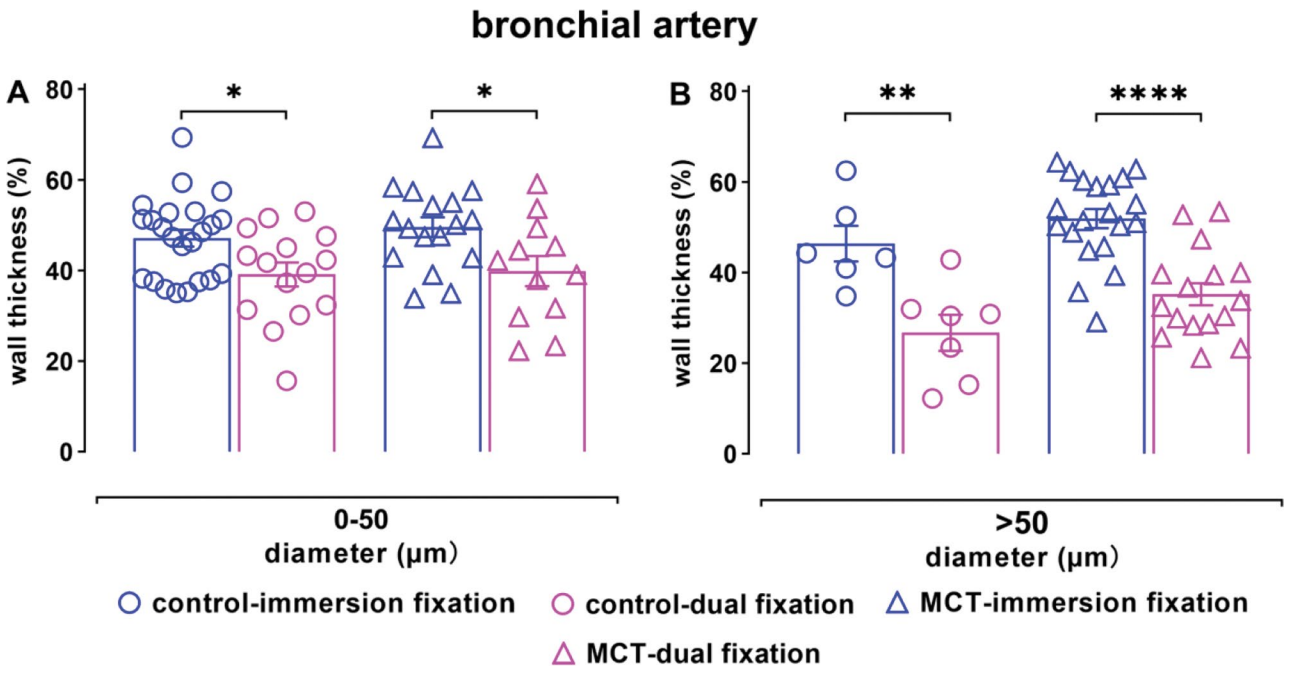

Fig. 6 The effect of fixation method on the evaluation of wall thickness of intrapulmonary arteries (snug against trachea) across varying diameters. The statistical comparisons of wall thickness in intrapulmonary arteries snug against trachea between dual fixation and immersion fixation in rats without or with MCT treatment (**A**-**B**), and between rats without or with MCT treatment by the same fixation method (**A**-**B**). * $P<0.05$, ** $P<0.01$, *** $P<0.001$, **** $P<0.0001$, $n=6$–23 pulmonary vessels from each of 6 rats for each group

MCT-treatment in these arteries revealed by the dual fixation than immersion fixation.

Discussion

This study introduces a novel lung tissue fixation method that significantly enhances the authenticity of pulmonary vascular morphology assessments in a rat model of PH. Our main findings indicate that this modified fixation method, combining ventilatory support and vascular perfusion, compared to the traditional immersion method, more effectively preserves lung tissue structure and pulmonary vascular morphology, offering a more precise representation of in vivo conditions. Being consistent with the conclusion revealed by male- and female-combined analysis (Fig. 2), data analysis stratifying by sex demonstrated the overall trend in better preservation of alveolar integrity by dual fixation than immersion fixation for both male and female rats (Figure. S5).

In the previous experiments on lung tissue fixation, the main focus was on a certain degree of protection for the airways and alveoli [5, 12], but timely fixation of intrapulmonary vessels and preservation of pulmonary vascular morphology were not addressed. These traditional tissue fixation methods, especially immersion fixation applied in rat models, may affect the apparent pulmonary vascular morphology in ex vivo lungs due to three main factors: the interruption of pulmonary circulation leading to decreased intravascular pressure and partial collapse of the pulmonary vessels [29], the loss of negative pressure in the thoracic cavity following thoracotomy, affecting the retractile force on the pulmonary vessels [11, 29], and hypoxic pulmonary vasoconstriction (HPV) due to the cessation of blood supply [30]. During the traditional lung tissue fixation process, the collapse of lung tissue and acute pulmonary hypoxia following thoracotomy led to strong vasoconstriction of pulmonary vessels and a decrease in their diameter. Smooth muscle cells transitioned from a circumferential flattened shape to an elliptical or columnar orientation perpendicular to the vessel wall, while elastic fibers underwent significant fluctuations [29–32]. This indicates that the traditional lung tissue fixation process results in an apparent thickening of the measured intrapulmonary vessel wall thickness compared to the actual pre-mortem thickness, and also causes previously open capillaries to collapse.

This study utilized a modified lung tissue fixation method. Initially, rats were maintained on a ventilator to sustain respiratory movements of the lung, thereby mitigating the effects of retractile forces on the lung tissue and vessels post-thoracotomy. Subsequently, perfusion pressure generated by the height of the liquid column was used to individually mimic the average pulmonary artery pressure and right heart output in vivo, fixing the pulmonary vessels to eliminate the impact of decreased vascular pressure and partial vessel collapse. Finally, tracheal ligation fixation was performed before lung tissue

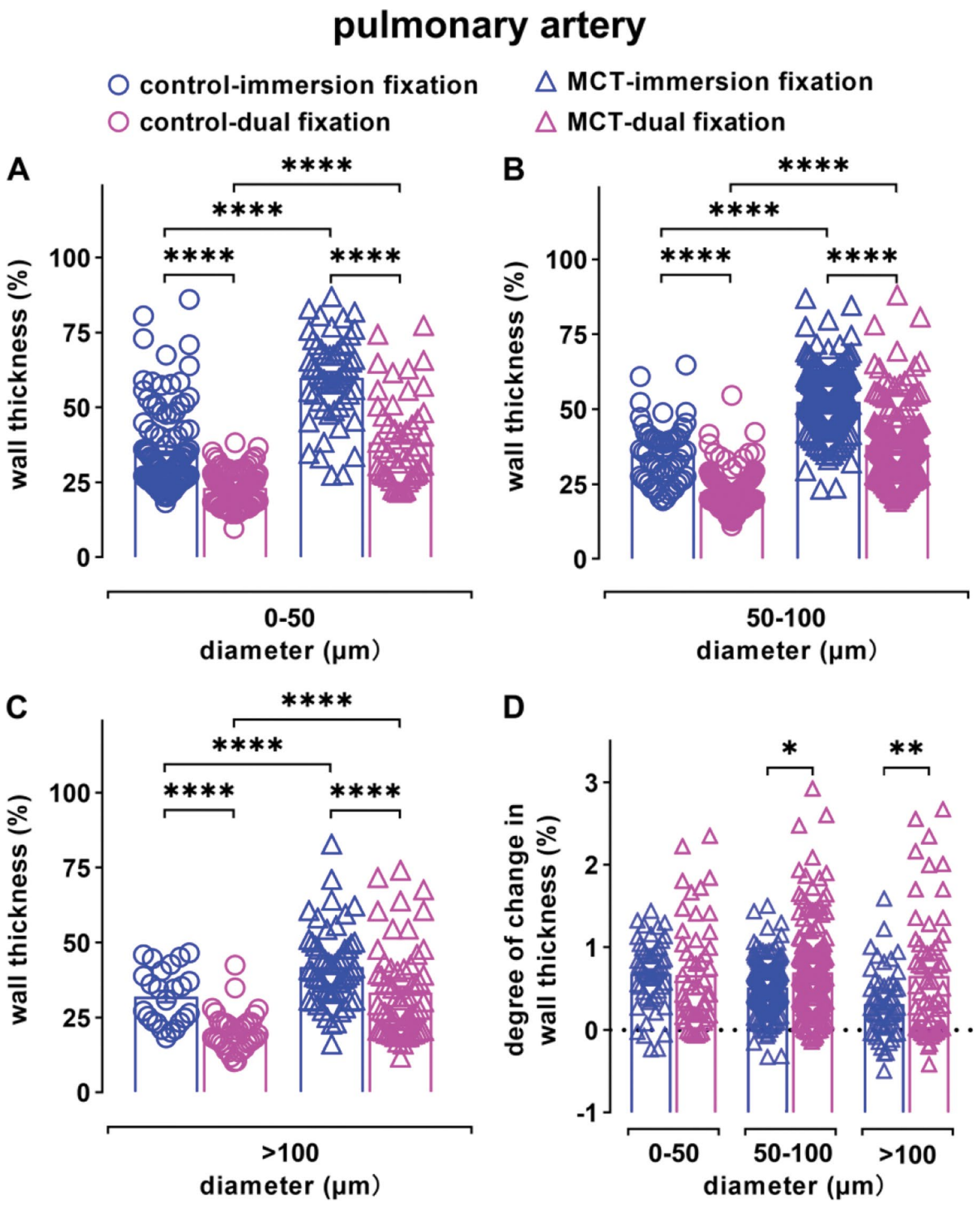

Fig. 7 The effect of fixation method on the wall thickness of intrapulmonary arteries (away from the trachea) across varying diameters. The statistical comparisons of wall thickness in intrapulmonary arteries away from trachea across different diameters between immersion fixation and dual fixation in rats without or with MCT treatment (**A**-**C**), and between rats without or with MCT treatment by the same fixation method (**A-C**). The effect of fixation method and MCT treatment on the alteration of wall thickness of intrapulmonary arteries away from trachea across varying diameters (**D**). * $P<0.05$, ** $P<0.01$, *** $P<0.001$, **** $P<0.0001$, $n=24$–167 pulmonary vessels from each of 6 rats for each group

dissection to prevent airway collapse after removal. Due to the use of an individualized method that simulates rat in vivo pulmonary arterial pressure and right ventricular output for intrapulmonary vascular perfusion fixation, we compared the effects of the modified fixation method with the traditional method on rat intrapulmonary vascular morphology. We assessed the ratio of opened/collapsed capillaries and the media thickness of intrapulmonary arteries and veins of varying diameters. Other studies have shown that gradually increasing pulmonary artery pressure for lung vascular perfusion fixation can cause discontinuities or breaks in the endothelial cell basement membrane in pulmonary capillaries under electron microscopy, though no significant changes were observed in endothelial cell junctions [33–35]. Therefore, we conducted an endothelial cell count analysis on non-capillary intrapulmonary vessels of various diameters to observe whether the modified fixation method, which simulates in vivo pulmonary artery pressure and right ventricular output for perfusion fixation, affects the integrity of endothelial cells in these vessels.

In our study, the modified method's superiority in preserving the integrity of lung tissue structure and capillary openness, providing a more accurate representation of in vivo conditions (Figs. 2 and 3), the wall thickness of intrapulmonary vessels fixed by the modified method was lower than that fixed by the traditional method across different vessels sizes and locations (Figs. 5, 6 and 7). Additionally, the modified method did not cause significant endothelial cell detachment (Fig. 4). Therefore, this novel lung tissue fixation method can more validly preserves the changes and complex spatial relationships within the pulmonary vasculature under in vivo conditions in rats.

A limitation of this study is that the modified fixation method does not eliminate the impact of HPV caused by interrupted blood supply. Given that HPV can be triggered within 5 to 10 s after hypoxia [30], acute hypoxia due to interrupted blood supply during sampling and fixation processes can lead to HPV. In conclusion, our study demonstrates that the modified lung tissue fixation method represents a methodological advancement in the morphological assessment of PH models, enabling more accurate and reliable histopathological evaluations in mechanistic and translational study of PH.

Supplementary Information

The online version contains supplementary material available at https://doi.org/10.1186/s12931-024-03091-8.

Supplementary Material 1

Acknowledgements
None.

Author contributions
QH established the study conception; QH, YX, PL, XS, RX and LZ devised the experiments; QH, YX, PL, XS, RX, LZ, YS, YX and JW executed the data analyses and interpretation; YX, WG, BL, TZ and TY performed the experiments; QH, LP, YX and XS wrote the manuscript; QH finalized the work. All authors approved the final version of article.

Funding
This study was supported by grants from the National Natural Science Foundation of China (grant numbers 82241014, 82130002, 82170068 and 82270060).

Data availability
No datasets were generated or analysed during the current study.

Declarations

Ethics approval and consent to participate
This study was approved by the Ethics Committee of Tongji Medical College, Huazhong University of Science and Technology.

Consent for publication
Not applicable.

Competing interests
The authors declare no competing interests.

Received: 10 November 2024 / Accepted: 31 December 2024
Published online: 18 January 2025

References

1. Humbert M, Kovacs G, Hoeper MM, et al. 2022 ESC/ERS guidelines for the diagnosis and treatment of pulmonary hypertension. Eur Respir J. 2023;61(1):2200879.
2. Mocumbi A, Humbert M, Saxena A, et al. Publisher correction: pulmonary hypertension. Nat Rev Dis Primers. 2024;10(1):5.
3. Gallardo-Vara E, Ntokou A, Dave JM, Jovin DG, Saddouk FZ, Greif DM. Vascular pathobiology of pulmonary hypertension. J Heart Lung Transpl. 2023;42(5):544–52.
4. Tuder RM. Pulmonary vascular remodeling in pulmonary hypertension. Cell Tissue Res. 2017;367(3):643–9.
5. Braber S, Verheijden KA, Henricks PA, Kraneveld AD, Folkerts G. A comparison of fixation methods on lung morphology in a murine model of emphysema. Am J Physiol Lung Cell Mol Physiol. 2010;299(6):L843–851.
6. Qu WS, Yin JY, Wang HM, Dong YS, Ding RG. A simple method for the formalin fixation of lungs in toxicological pathology studies. Exp Toxicol Pathol. 2015;67(10):533–8.
7. Matulionis DH. Lung deformation and macrophage displacement in smoke-exposed and normal mice (Mus musculus) following different fixation procedures. Virchows Arch Pathol Anat Histopathol. 1986;410(1):49–56.
8. Bachofen H, Ammann A, Wangensteen D, Weibel ER. Perfusion fixation of lungs for structure-function analysis: credits and limitations. J Appl Physiol Respir Environ Exerc Physiol. 1982;53(2):528–33.
9. de Visser YP, Walther FJ, Laghmani el H, Boersma H, van der Laarse A, Wagenaar GT. Sildenafil attenuates pulmonary inflammation and fibrin deposition, mortality and right ventricular hypertrophy in neonatal hyperoxic lung injury. Respir Res. 2009;10(1):30.
10. D'hulst AI, Vermaelen KY, Brusselle GG, Joos GF, Pauwels RA. Time course of cigarette smoke-induced pulmonary inflammation in mice. Eur Respir J. 2005;26(2):204–13.
11. Hausmann R, Bock H, Biermann T, Betz P. Influence of lung fixation technique on the state of alveolar expansion-a histomorphometrical study. Leg Med (Tokyo). 2004;6(1):61–5.
12. van Kuppevelt TH, Robbesom AA, Versteeg EM, Veerkamp JE, van Herwaarden CL, Dekhuijzen PN. Restoration by vacuum inflation of original alveolar dimensions in small human lung specimens. Eur Respir J. 2000;15(4):771–7.

13. Sztuka K, Jasińska-Stroschein M. Animal models of pulmonary arterial hypertension: a systematic review and meta-analysis of data from 6126 animals. Pharmacol Res. 2017;125(Pt B):201–14.
14. Xiao R, Su Y, Feng T, et al. Monocrotaline induces endothelial injury and pulmonary hypertension by targeting the extracellular calcium-sensing receptor. J Am Heart Assoc. 2017;6(4):e004865.
15. Xiao R, Luo S, Zhang T, et al. Peptide blocking self-polymerization of extracellular calcium-sensing receptor attenuates hypoxia-induced pulmonary hypertension. Hypertension. 2021;78(5):1605–16.
16. Tan R, Li J, Liu F, et al. Phenylalanine induces pulmonary hypertension through calcium-sensing receptor activation. Am J Physiol Lung Cell Mol Physiol. 2020;319(6):L1010–20.
17. Zhu L, Xiao R, Zhang X, Lang Y, Liu F, Yu Z, Zhang J, Su Y, Lu Y, Wang T, et al. Spermine on endothelial extracellular vesicles mediates smoking-induced pulmonary hypertension partially through calcium-sensing receptor. Arterioscler Thromb Vasc Biol. 2019;39(3):482–95.
18. Liu B, Wei YP, Fan X, et al. Calcium sensing receptor variants increase pulmonary hypertension susceptibility. Hypertension. 2022;79(7):1348–60.
19. Hsia CC, Hyde DM, Ochs M, Weibel ER, ATS/ERS Joint Task Force on Quantitative Assessment of Lung Structure. An official research policy statement of the American Thoracic Society/European Respiratory Society: standards for quantitative assessment of lung structure. Am J Respir Crit Care Med. 2010;181(4):394–418.
20. Weibel ER. Lung morphometry: the link between structure and function. Cell Tissue Res. 2017;367(3):413–26.
21. Auten RL Jr, Mason SN, Tanaka DT, Welty-Wolf K, Whorton MH. Anti-neutrophil chemokine preserves alveolar development in hyperoxia-exposed newborn rats. Am J Physiol Lung Cell Mol Physiol. 2001;281(2):L336–344.
22. Yang M, Chen Y, Huang X, Shen F, Meng Y. ETS1 ameliorates hyperoxia-induced bronchopulmonary dysplasia in mice by activating Nrf2/HO-1 mediated ferroptosis. Lung. 2023;201(4):425–41.
23. Jung K, Schlenz H, Krasteva G, Mühlfeld C. Alveolar epithelial type II cells and their microenvironment in the caveolin-1-deficient mouse. Anat Rec (Hoboken). 2012;295(2):196–200.
24. Roggendorf W, Cervós-Navarro J. Ultrastructure of arterioles in the cat brain. Cell Tissue Res. 1977;178(4):495–515.
25. Rhodin JA. The ultrastructure of mammalian arterioles and precapillary sphincters. J Ultrastruct Res. 1967;18(1):181–223.
26. Townsley MI. Structure and composition of pulmonary arteries, capillaries, and veins. Compr Physiol. 2012;2(1):675–709.
27. Hashizume H, Tango M, Ushiki T. Three-dimensional cytoarchitecture of rat pulmonary venous walls: a light and scanning electron microscopic study. Anat Embryol (Berl). 1998;198(6):473–80.
28. Roberts JC, McCrossan MV, Jones HB. The case for perfusion fixation of large tissue samples for ultrastructural pathology. Ultrastruct Pathol. 1990;14(2):177–91.
29. Buyssens N, van den Bossche R, de Meyer G, Herman AG. The influence of collapse of the lung parenchyma on the morphology of pulmonary blood vessels in the rat. Acta Anat (Basel). 1996;155(1):22–8.
30. Dunham-Snary KJ, Wu D, Sykes EA, et al. Hypoxic pulmonary vasoconstriction: from molecular mechanisms to medicine. Chest. 2017;151(1):181–92.
31. Schwenke DO, Pearson JT, Umetani K, Kangawa K, Shirai M. Imaging of the pulmonary circulation in the closed-chest rat using synchrotron radiation microangiography. J Appl Physiol (1985). 2007;102(2):787–93.
32. Hirschman JC, Boucek RJ. Angiographic evidence of pulmonary vasomotion in the dog. Br Heart J. 1963;25(3):375–81.
33. Tsukimoto K, Mathieu-Costello O, Prediletto R, Elliott AR, West JB. Ultrastructural appearances of pulmonary capillaries at high transmural pressures. J Appl Physiol (1985). 1991;71(2):573–82.
34. West JB, Mathieu-Costello O. Stress failure of pulmonary capillaries: role in lung and heart disease. Lancet. 1992;340(8822):762–7.
35. Costello ML, Mathieu-Costello O, West JB. Stress failure of alveolar epithelial cells studied by scanning electron microscopy. Am Rev Respir Dis. 1992;145(6):1446–55.

Publisher's note